RESEARCH ARTICLE

Association of TNF-α, IGF-1, and IGFBP-1 levels with the severity of osteopenia in mice with nonalcoholic fatty liver disease

Tong-Hao Wang[1†], Jian-Biao Li[2†], Yong-Gang Tian[1], Jin-Xin Zheng[1], Xiao-Dong Li[1] and Shu-zhang Guo[1*]

Abstract

Backgrounds Nonalcoholic fatty liver disease (NAFLD) exhibits a close association with osteoporosis. This work aims to assess the potential effects of NAFLD on the progression of osteopenia in animal models.

Methods Forty-eight C57BL/6 female mice were randomly divided to wild-type (WT) group and high-fat diet (HFD) group. The corresponding detections were performed after sacrifice at 16, 24 and 32 weeks, respectively.

Results At 16 weeks, an remarkable increase in body weight and lipid aggregation in the hepatocytes of HFD group was observed compared to the WT group, while the bone structure parameters showed no significant difference. At 24 weeks, the levels of TNF-α and IL-6 in NAFLD mice were significantly increased, while the level of osteoprotegerin mRNA in bone tissue was decreased, and the level of receptor activator of nuclear factor Kappa-B ligand mRNA was increased. Meanwhile, the function of osteoclasts was increased, and the bone microstructure parameters showed significant changes. At 32 weeks, in the HFD mice, the mRNA levels of insulin-like growth factor-1 (IGF-1), runt-related transcription factor 2, and osterix mRNA were reduced, while the insulin-like growth factor binding protein-1 (IGFBP-1) level was increased. Simultaneously, the osteoblast function was decreased, and the differences of bone structure parameters were more significant, showing obvious osteoporosis.

Conclusions The bone loss in HFD mice is pronounced as NAFLD progresses, and the changes of the TNF-α, IL-6, IGF-1, and IGFBP-1 levels may play critical roles at the different stages of NAFLD in HFD.

Main Points

- Bone loss in the HFD mice becomes increasingly apparent with NAFLD progression.
- The changes of the TNF-α, IL-6, IGF-1, and IGFBP-1 levels are important at the different stages of NAFLD in the HFD mice.

Keywords Nonalcoholic fatty liver disease, Osteoporosis, Tumor Necrosis factor-alpha, Insulin-Like growth factor I, Insulin-Like growth factor binding protein-1

---

†Tong-Hao Wang and Jian-Biao Li contributed equally to this work.

*Correspondence:
Shu-zhang Guo
guoshuzhang99@163.com
Full list of author information is available at the end of the article

Wang *et al. Journal of Orthopaedic Surgery and Research*   (2023) 18:915

Page 2 of 11

Introduction

As one of the most common chronic metabolic liver disorders, nonalcoholic fatty liver disease (NAFLD) is a clinicopathological syndrome characterized by excessive deposition of fat in hepatocytes, including simple fatty liver disease (SFL), nonalcoholic steatohepatitis (NASH), and associated cirrhosis. Multiple factors contribute to the pathogenesis of NAFLD, such as insulin resistance (IR) and overweight. In a recent epidemiological study, NAFLD is confirmed to be related to osteoporosis [1], sharing common risk factors, including aging, inappropriate lifestyles and sex hormone deficiency, indicating that they might be related in some way [2].

With several publications supporting the correlation between a reduced bone mineral density (BMD) and NAFLD [3, 4]. While it is conflict to use overweight and IR to explain this phenomenon. Recently, whether there is a positive correlation between bodyweight and bone mass has been discussed in obese-related studies [5]. Overweight and the increased body mass index (BMI) are related to bone mass because the increase in weight and fat during exercise cause bones to withstand greater forces and promotes an increase in bone density [6]. Another study found that IR was associated with the increased BMD, while this increase did not affect the serum cytokine levels [7]. Therefore, the changes of bone microstructure and BMD in NAFLD remain intensely debated.

NAFLD is a multifactorial disease that is thought to be caused by multiple genetic and environmental factors. The pathogenesis of NAFLD is explained by the '2-hit' hypothesis [8], and the 'first hit' was considered to participate in accumulation of triglyceride (TG) in hepatocytes or steatosis. It is reported that the 'second hit' is closely linked to oxidative stress and inflammatory cytokines. The accumulation of IR and TG, chronic inflammatory processes, vitamin D deficiency, and insulin-like growth factor-1 (IGF-1) reduction play important roles in the pathogenesis of NAFLD, which may be related to osteoporosis.

Herein, we aims to analyze the changes in bone microarchitecture and mineralization over time by microcomputed tomography (micro-CT) in a mouse model of NAFLD induced by a high-fat diet (HFD) and hereby address the following aims: (1) investigate the changes of bone microstructure and pathogenesis in the progression of NAFLD; (2) investigate the role of TNF-α and IGF-1 during osteoporosis in NAFLD mice.

Materials and methods

Animals

Forty-eight 6-week-old wild-type C57BL/6 female mice (weight, 20 ± 2 g) were purchased from Vital River Laboratories (Beijing, China). All the mice were housed in a suitable environment with a temperature of 20–22 °C, humidity of 50–60% in light/dark cycle for 12 h/12 h. Mice were free to eat and drink, and the bodyweight was measured during the study period. The animal experimental procedures were approved by the Experimental Animal Committee at The Third Central Hospital of Tianjin. All the experiments performed in this study were approved and conducted according to standard guidelines of the Institutional animal ethical committee (2020–142). Following adaptation for 1 week. The mice were randomly divided into two groups: wild-type C57BL/6 mice (WT group, $n = 24$); wild-type C57BL/6 mice with HFD (HFD group, $n = 24$). HFD (D12492, Research Diet, USA) is made up of protein (20 kcal%), carbohydrates (20 kcal%), and fat (60 kcal%). At 16 weeks, 24 weeks and 32 weeks, eight mice in each group were anaesthetized with sodium pentobarbital (50 mg/kg, intraperitoneal injection) and decapitated. Blood, liver, femur and tibiae were collected and stored for later use.

Measurement of body and organ weight

The weight of mice was measured at the end of 16, 24 and 32 weeks. After the mice were sacrificed, the liver of the mice was extracted, fully washed by normal saline, drained and then, weighed with an electronic balance. Liver index were calculated using the liver weight and the equivalent body weight of respective animals.

Biochemical marker analysis

After the mice were sacrificed, blood samples were collected from the eyeballs, and after static coagulation for 15–20 min, serum was separated by rotating at 4000 rpm for 10 min and stored at -20 °C. Blood biochemical markers such as Alanine transaminase (ALT), serum glucose (GLU), aspartate aminotransferase (AST), triglycerides (TG) levels, and total cholesterol (TC) were detected by a Hitachi automatic biochemical analyzer (HITACHI, Japan). In addition, the IL-6 and TNF-α levels in serum were measured by enzyme-linked immunosorbent assay (ELISA) kits produced by Shanghai Fusheng Industrial Co., Ltd. (Shanghai, China). The test procedures were executed according to the manufacturers' instructions. Serum GLU and insulin were analyzed using a glucometer (Bayer, Germany) and ELISA kit (Roche, Switzerland), respectively. Serum IGF-1 and insulin-like growth factor binding protein-1(IGFBP-1) were determined using

Wang *et al. Journal of Orthopaedic Surgery and Research*   (2023) 18:915

Page 3 of 11

a radioimmunoassay kit (ALPCO, Windham, NH) and ELISA kit (Insight Genomics, Falls Church, VA), respectively. Total serum 25-hydroxyvitamin D (25(OH)D) level was measured using liquid chromatography mass spectroscopy (LC–MS).

Liver and bone histological analysis

To investigate liver steatosis and bone structure changes, liver sections and the right tibiae sections from the same part of each animal were fixed in 4% paraformaldehyde for 24 h, dehydrated with alcohol gradient, embedded in paraffin wax, and stained with hematoxylin and eosin (HE) for pathological examination. The histological results showed that the adipose area of liver tissue was more than 1/3, indicating that the NAFLD animal model was successfully established.

Micro-CT detection of bone microstructure

The right femur of mice was subsequently isolated and immobilized at 4 °C PBF (pH 7.4) for 24 h. The 70% ethanol was used to dehydrate each sample for 48 h and then, removed into a 8 mL tube filled with 70% ethanol to measure bone microarchitecture and BMD using micro-CT (Skyscan 1076 Micro-CT System; Skyscan, Aartselaar, Belgium). All scans were performed using X-ray energy at 50 kV and 200 μA, and the samples were scanned over one entire 360° rotation, with an exposure time of 2000 ms/frame. An isotopic resolution of 9.0 μm × 9.0 μm × 9.0 μm voxel size was selected to reveal the microstructure of the mouse trabecula. The incremental angle around the sample was set as 0.5° to obtain 1000 two-dimensional images. Mimics 17.0 (Materialize Company, Belgium) software was used for 3D image reconstruction and analysis. The epiphyseal trabeculae and cortical bones were selected as areas of interest for analysis. BMD, trabecular separation (Tb.Sp), bone volume ratio (BV/TV), trabecular thickness (Tb.Th), trabecular number (Tb.N), connectivity density (Conn.D), and cortical thickness (C.Th) were used for the morphological measurements and analysis. Bone mineral density was divided into tissue BMD (tBMD) and volumetric BMD (vBMD) by microscopic CT analysis.

Analysis of born turnover markers in serum

Serum levels of tartrate-resistant acid phosphatase (TRAP), c-terminal crosslinked telopeptides of type I collagen (CTX-1), n-terminal propeptide of type I procollagen (PINP), and alkaline phosphatase (ALP) were analyzed using commercially available ELISA kits (Yanjin Biotech Company Limited, Shanghai), and the values were read using a double beam spectrophotometer.

Three-point bending experiment of femur

The left femur from experimental animals was removed, and the biomechanical properties were evaluated by a three-point bending test on an electronic universal machine (INSTRON 5584). The loading speed is set at 2 mm/min, the lower span is 1 cm, and the sample is loaded at a constant speed until the sample is completely broken. The test parameters include Maximum loading (N), Stiffness (N/mm), Maximum deflection (mm), and Elastic modulus (Gpa).

Real-time polymerase chain reaction (RT-PCR) analysis

The left tibiae of both groups of mice were dissolved and fully homogenized with an electric homogenizer and further mixed with a ribonucleic acid (RNA) reagent and the RNA was extracted according to the standard procedures [9]. The extracted RNA was detected on the spectrophotometer, and then RNA reverse transcription was performed according to the kit procedure (TaKaRa Company, Japan). RT-PCR was performed, and the mRNA expression of Runx2, Osx, OPG, and RANKL was determined and normalized to the house-keeping gene (β-actin). The PCR analysis was performed under the following conditions (initial denaturation at 95 °C for 15 s, annealing at 64 °C for 30 s, primer extension at 72 °C for 30 s) about 40–45 cycles.

Statistics

SPSS 22.0 (IBM Corp., Armonk, NY, USA) was used for all statistical comparisons. All data were expressed as means ± standard deviation (SD). *T* test was used to compare the mean of the two samples, and one-way ANOVA with repeated measures was used to identify significant differences between multiple groups. The two-tailed test was used, and $P < 0.05$ indicated significant differences.

Results

Pathological changes of liver in mice with NAFLD

After 16, 24 and 32 weeks of feeding, the body weight of all experimental animals was gradually increased, and the body weight of HFD group was significantly increased compared with that of control group (WT group) ($P < 0.05$, Fig. 1A). There was no significant difference in liver weight at all ages in WT group. However, compared with WT group, liver weight and liver index in HFD group were significantly increased, with the most significant increase at 16 weeks ($P < 0.01$) and decrease at 24 weeks compared with 16 weeks ($P < 0.05$), while increased again at 32 weeks ($P < 0.01$). The liver weight of HFD group at 24 weeks was lower than that at 16 weeks and 32 weeks, showing significant differences ($P < 0.05$, Fig. 1B). The liver index of HFD group was also decreased
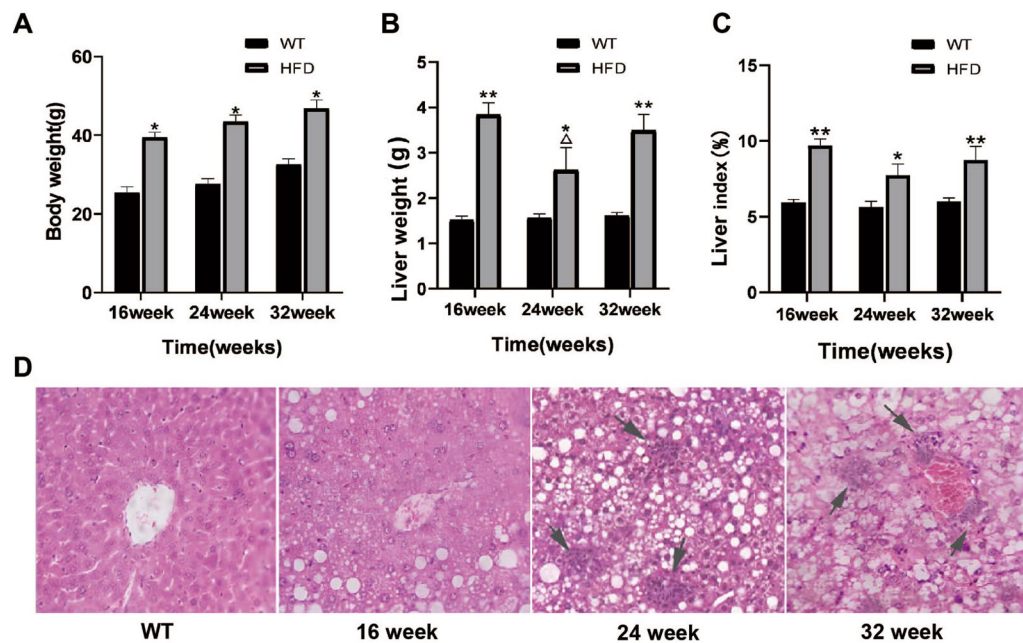
Fig. 1 Pathological changes of liver in mice with NAFLD. Comparison of body weight (**A**), liver weight (**B**) and liver index (**C**) in each group of mice. **D** HE staining on liver tissues in mice. *$P < 0.05$, **$P < 0.01$ versus WT group; $\triangle P < 0.05$, versus HFD group at 16 week and 32 week

at 24 weeks, but no significant difference was observed between this time point and others (Fig. 1C). Histological examination of HE-stained liver sections revealed the progression of macrovesicular steatosis at 16 weeks and inflammation cell infiltration at 24 and 32 weeks in the HFD mice compared with the WT mice, in a time-dependent manner (Fig. 1D).

Serum biochemical analysis of mice with NAFLD

At 16 weeks, the levels of TG, TC and insulin in HFD group were significantly higher than those in WT group ($P < 0.01$, Fig. 2A–C), which was consistent with NAFLD characteristics, indicating that HFD mouse model was successfully constructed. In contrast, there was no significant difference in AST and ALT levels between the two groups. At 24 weeks and 32 weeks, the levels of TC, TG, ALT, AST and insulin in HFD group were higher than those in WT group, with statistical significance ($P < 0.05$), and the change of ALT was the most significant ($P < 0.01$). At 32 weeks, the TC level in HFD group was significantly higher than that in other age groups. Compared with the control group, GLU level in HFD group was slightly increased at all ages, but the difference was not statistically significant (Fig. 2 D–F).

Changes of biomechanical properties and bone structures of mice with NAFLD

The results of three-point mechanical test showed that the maximum load was slightly increased and the bending stiffness, maximum deflection and bending elastic modulus were slightly decreased in HFD group at 16 weeks than that of control group, but there was no significant statistical difference, indicating that the femur of mice in HFD group could bear higher weight at 16 weeks, but the toughness was poor. At 24 weeks and 32 weeks, all parameters showed significant decline, and there was a statistical difference than that of control group ($P < 0.05$, Fig. 3A–D), indicating that the bone strength and toughness of mice in HFD group were significantly reduced. In addition, at 16 weeks of HFD group, bone trabeculae was damaged, and the bone damage in HFD group was gradually aggravated in the progression of NAFLD. (Fig. 3E). These data suggest a significant correlation between the progression of NAFLD and the occurrence of osteoporosis.

Morphology and structural parameters of distal femur

Compared to the WT group, the microstructure of distal femur bone in the HFD group did not change significantly at 16 weeks. From 24 to 32 weeks, the metaphyseal structure of mice in the HFD group had significant changes, and the injuries were aggravated in the progression of disease (Fig. 4A, B). The differences between the HFD and WT group at 16 weeks in the structural parameters or BMD had no significance except Tb.Sp and c.Th. At 24 and 32 weeks, the Tb.N, BV/TV, Tb.Th, c.Th, Conn.D, vBMD, and tBMD in the HFD group was significantly lower than the WT group, whereas the Tb.Sp was
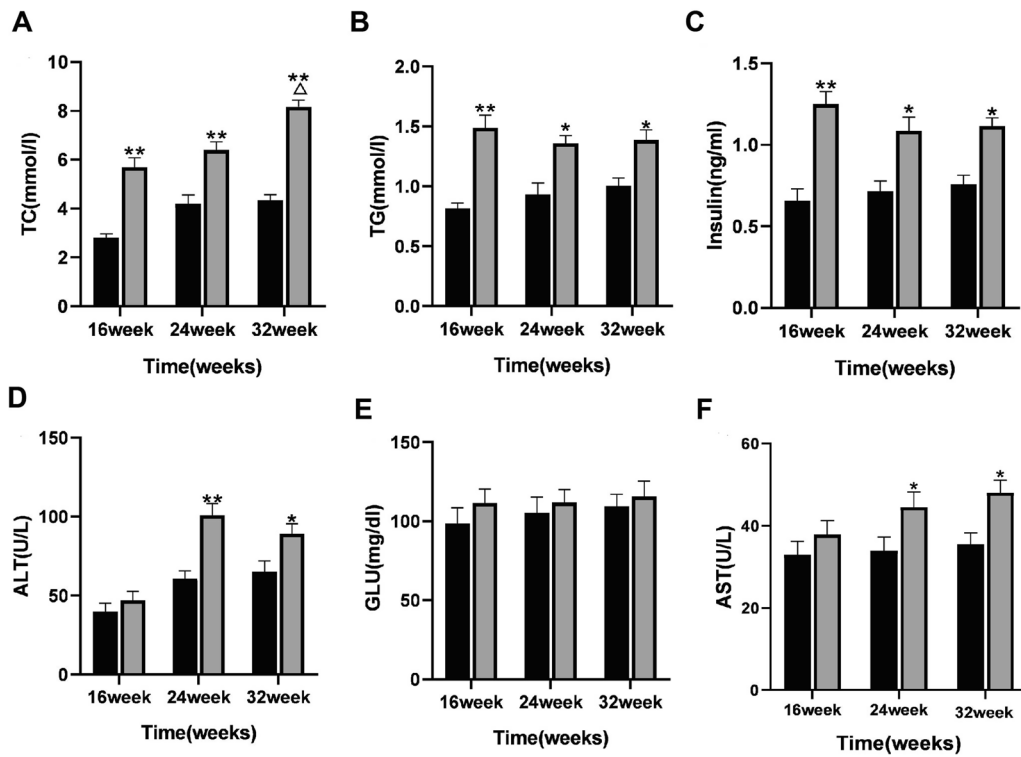
Fig. 2 Comparison of serum biochemical detection in mice with NAFLD. Comparison of TC (**A**), TG (**B**), Insulin (**C**), ALT (**D**), GLU (**E**), and AST (**F**) in each group of mice. $*P < 0.05$, $**P < 0.01$ versus WT group; $^{\triangle}P < 0.05$ versus 16 week or 24 week group. Scale bar: 50 μm
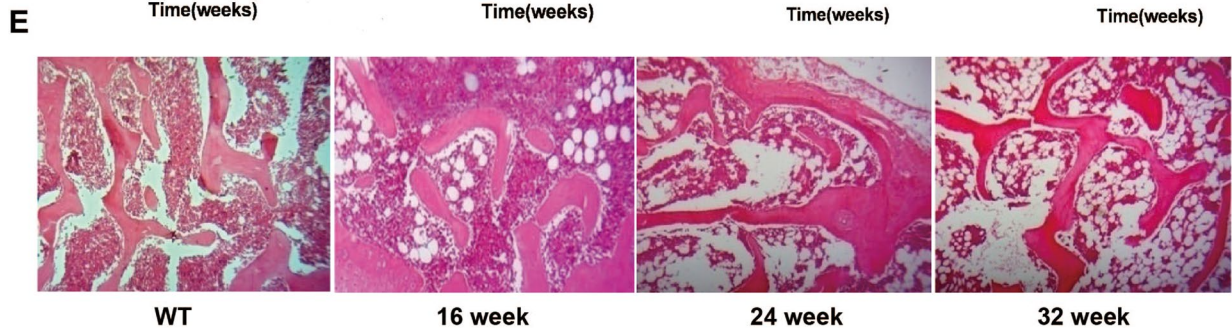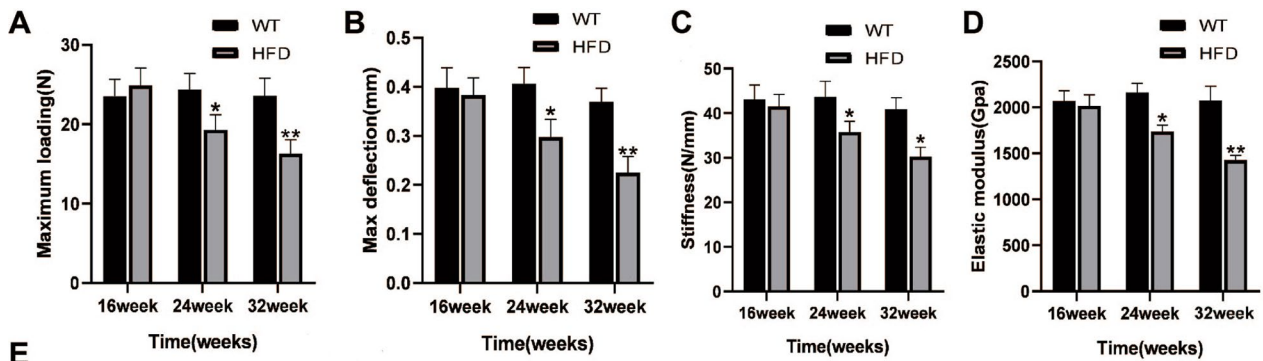

Fig. 3 Changes of biomechanical properties and bone structures of mice with NAFLD. Comparison of maximum loading (**A**), max deflection (**B**), stiffness (**C**), and elastic modulus (**D**) in each group of mice. **E** HE staining on tibia tissues in mice. $*P < 0.05$, $**P < 0.01$ versus WT group
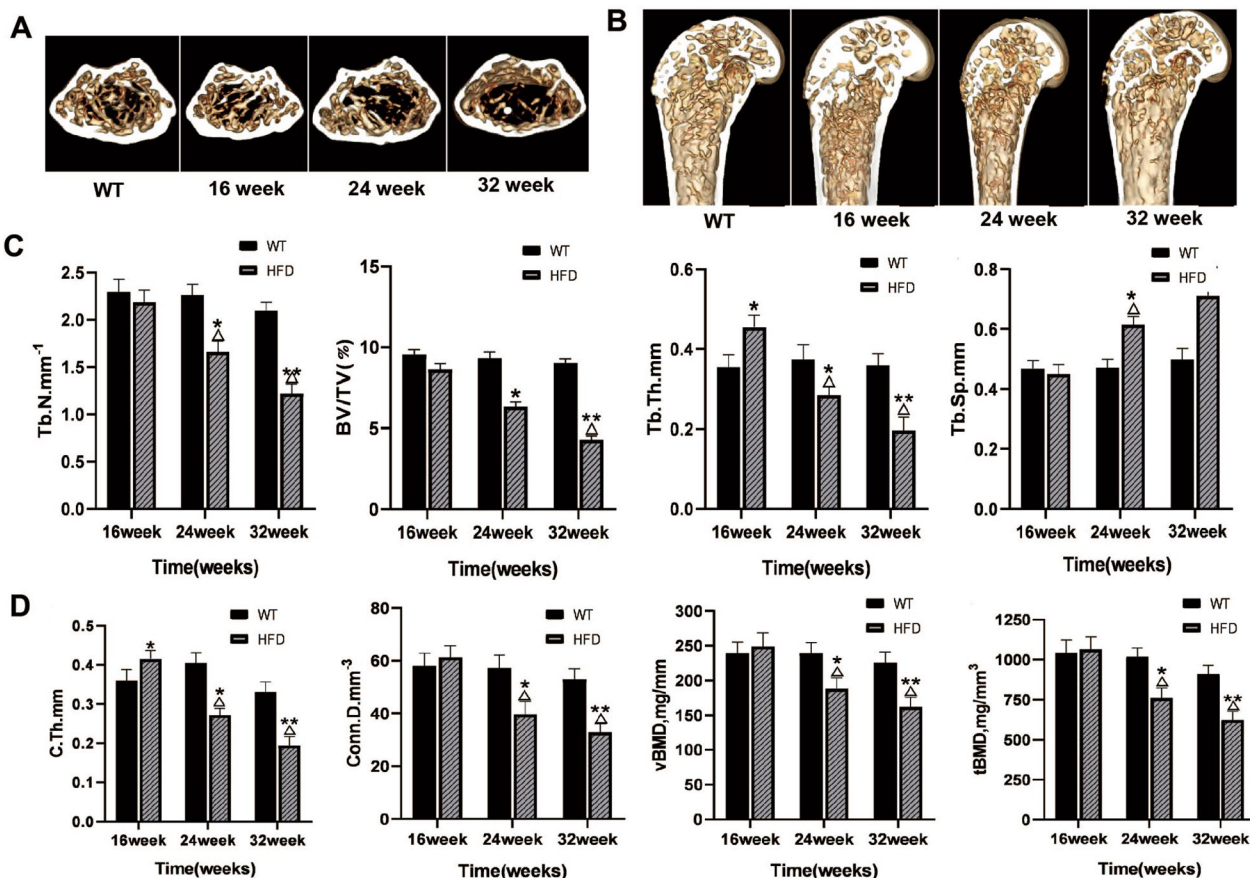
Fig. 4 Morphology and structural parameters of the distal femur. **A**, **B** Three-dimensional morphological changes of bone microstructure in distal femurs and trabeculae and cortical thickness in distal femurs of mice in two groups. **C**, **D** Structural features of trabecular bone and cortical bone in the the distal femur of mice at 16, 24 and 32 weeks. *$P < 0.05$, **$P < 0.01$ versus WT group; $^{\triangle}P < 0.05$ versus HFD group at 16 weeks

remarkably greater in the HFD group ($P < 0.05$ or $P < 0.01$, Fig. 4C, D). In the HFD group, the respective changes of all the metaphyseal structural parameters from 24 to 32 weeks were significant, suggesting the development of osteopenia with the aggravation of NAFLD in HFD group.

Alterations of TNF-α, IL-6, IGF-1, IGFBP-1, and 25-OH VitD in the serum of mice
As shown in Fig. 5A, B, there was no significant difference of TNF-α and IL-6 levels between WT and HFD group at 16 weeks. At 24 weeks, the levels of TNF-α and IL-6 were significantly higher than those in WT group ($P < 0.01$), but the changes decreased at 32 weeks. Compared with WT group, IGF-1 level in HFD group was decreased at 24 weeks ($P < 0.05$), and the difference was more significant at 32 weeks ($P < 0.01$, Fig. 5C). It was found that the IGFBP-1 level was significant lower in HFD group than that in WT group at 16 weeks ($P < 0.05$, Fig. 5D), but no significant difference was observed between the two groups at 24 weeks ($P > 0.05$). At 32 weeks, the IGFBP-1

level increased further in the HFD group, which was significantly higher than that of 24 weeks (Fig. 5D). The differences between the HFD group and WT group on 25-OH VitD level was not significant at any time point ($P > 0.05$, Fig. 5E).

Changes of serum bone turnover markers in mice
To evaluate the bone metabolism of HFD mice, CTX-1, TRACP5b, PINP and ALP in serum of mice were detected by ELISA assay. Compared to the mice in WT group, the levels of PINP and ALP in HFD group were increased at 16 weeks, but the difference was not statistically significant, indicating that osteogenic function of HFD mice was enhanced at 16 weeks, which might be related to the increased body load caused by weight increase. Compared with WT group, serum TRACP5b and CTX-1 contents of HFD mice were significantly increased at 24 weeks ($P < 0.01$) and decreased at 32 weeks ($P < 0.05$) compared with 24 weeks, indicating that osteoclast function was strongest at 24 weeks and decreased at 32 weeks (Fig. 6A, B). The contents of PINP
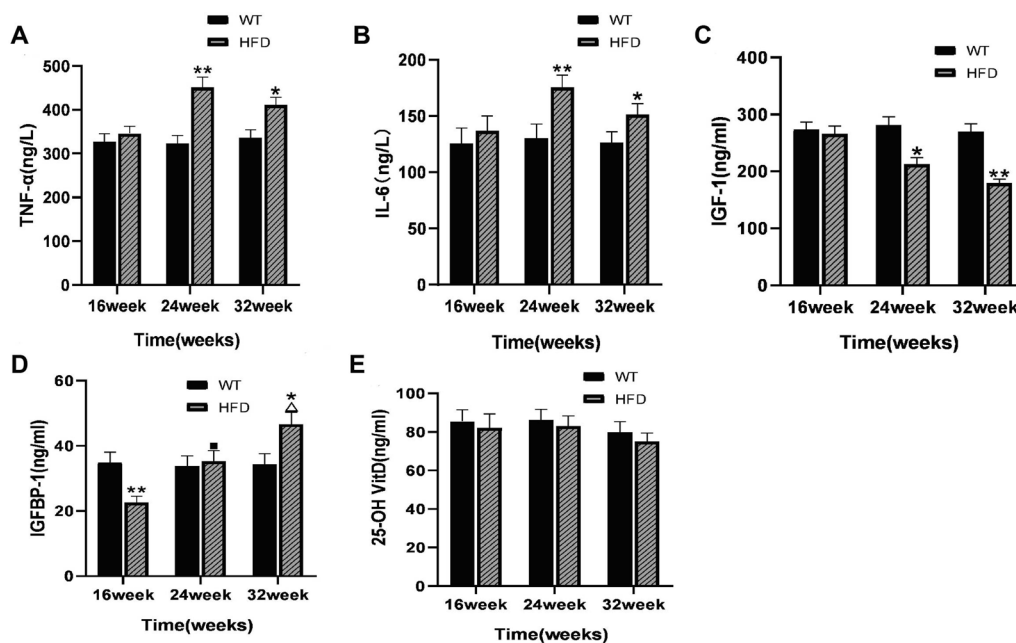
Fig. 5 Detection of serum cytokines in mice. The serum levels of TNF-α (**A**), IL-6 (**B**), IGF-1 (**C**), IGFBP-1 (**D**) and 25-OH VitD (**E**) in mice at 16, 24 and 32 weeks were measured by ELISA. *$P < 0.05$, **$P < 0.01$ versus WT group; ■$P > 0.05$ versus WT group; △$P < 0.05$ versus HFD group at 24 weeks; △$P < 0.05$ versus HFD group at 16 weeks
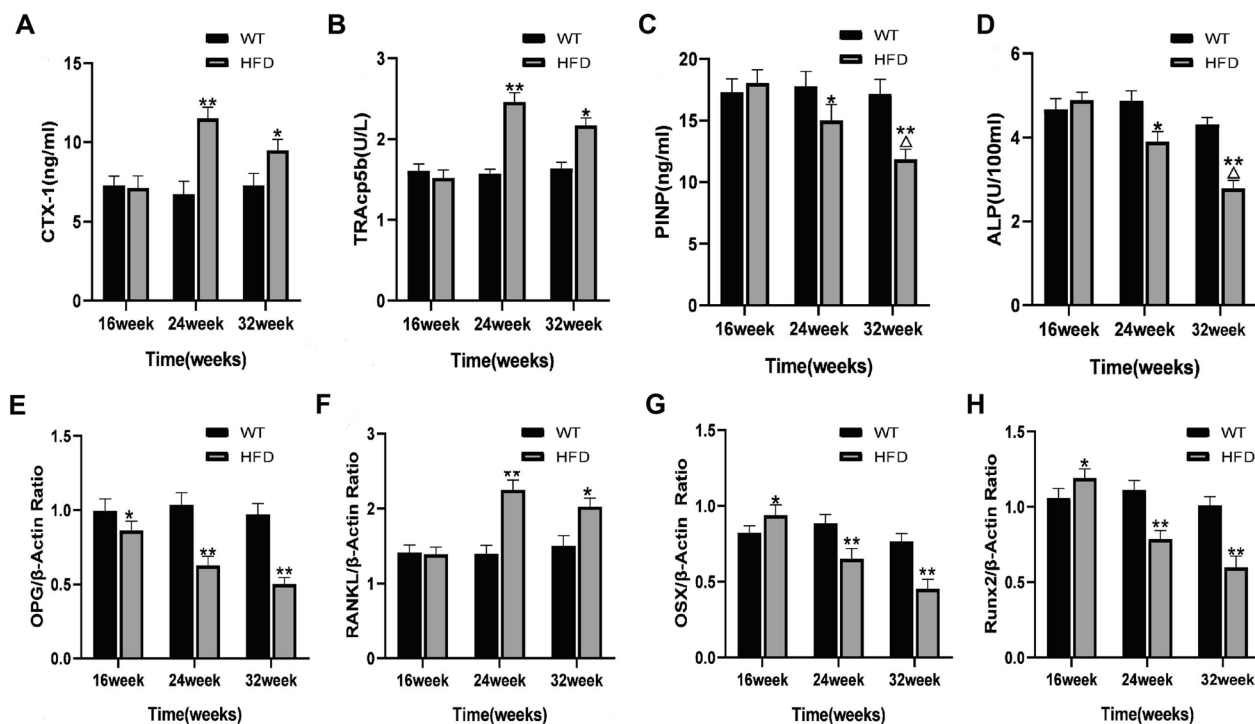

Fig. 6 Changes of serum bone turnover markers in mice. **A**–**D** The serum levels of CTX-1, TRACP5b, PINP and ALP in mice of each groups at 16, 24 and 32 weeks were evaluated by ELISA. **E**–**H** The mRNA expression levels of Runx2, Osx, OPG, and RANKL in tibiae of each groups at 16, 24 and 32 weeks were detected by RT-PCR. *$P < 0.05$, **$P < 0.01$ versus WT group; △$P < 0.05$ versus HFD group at 24 weeks

and ALP decreased significantly at 24 weeks ($P < 0.05$) and decreased more significantly at 32 weeks ($P < 0.01$), indicating that with the progression of HFD mice, osteoblastic function was gradually weakened and osteoporosis appeared (Fig. 6C, D).

At 16 weeks, the OPG mRNA level in mouse tibiae of HFD group was decreased, and the mRNA expressions of OSX and Runx2 were increased, while the RANKL mRNA level did not change when compared to the WT group ($P < 0.05$, Fig. 6E–H), suggesting that osteoblast function of mice in HFD group was enhanced, which was considered to be associated with the increase in body weight load. From 24 to 32 weeks, the mRNA levels of OPG, OSX and Runx2 in tibiae of HFD group were decreased in comparison to the WT group, while the RANKL mRNA level showed opposite results ($P < 0.01$, Fig. 6E–H), indicating that osteoblast function was gradually weakened with the aggravation of NAFLD.

Discussion

Nowadays, growing evidence indicated that NALFD had a close relationship between NAFLD and bone health. However, to date, it remains highly controversial about the relationship between NAFLD and bone health [10]. A HFD containing 60% energy from fat induced NAFLD-resulted metabolic changes in C57BL/6 mice, which can tightly represent human metabolic syndrome, including dyslipidemia, inflammation, and obesity [11]. Li et al. [12] found that the liver lipid content peaked at 16 weeks, significantly promoted the level of pro-inflammatory cytokines at 24 weeks, and fibrosis increased subsequently in some mice at 32 weeks. Studies have found that the prevalence of NAFLD in women increases significantly with age, and the moderate or severe but not mild NAFLD is independently associated with osteoporosis, indicating that the severity of NAFLD in women may be associated with osteoporosis [13, 14]. Based on the above studies, we investigated the serum biochemistry, cytokines and bone microstructure of female mice with NAFLD at 16, 24 and 32 weeks. The Changes of GLU levels could rule out bone loss caused by diabetes.

Histopathological data showed that the bone tissue destruction occurred and gradually worsened with the aggravation of NAFLD in HFD mice. At 16 weeks, the BMD of HFD mice was increased, which was thought to be related to the increase in body load caused by weight increase. Overweight is associated with bone mass to a certain extent, because the increase in weight and fat during exercise makes bones bear greater force, promoting the increase in bone density [6]. However, the bending stiffness and elastic modulus of the bone were decreased in HFD group, indicating that the bone quality was not high and the toughness was poor. At 24 weeks and 32 weeks, the distal femur of mice in HFD group showed significant changes, suggesting that the osteoporosis gradually appeared in HFD group mice with the aggravating of NAFLD.

The second stage of NAFLD is NASH, and insulin resistance is the main pathophysiological change in this stage. Insulin resistance can cause adipose tissue to secrete leptin, IL-6, TNF-α and other adipocytokines, and interact with these factors to cause the 'second hit' [15], in which TNF-α plays a key role in this stage [16]. The increase in serum TNF-α level directly stimulates the maturation and activation of osteoclasts and induces IL-6 release from mature osteoclasts. Importantly, IL-6 facilitates the bone resorption and differentiation of osteoclast precursors [17]. TNF-α and IL-6 jointly promote the formation of osteoclasts and bone resorption [18]. In diet-induced NAFLD rodents, RANKL is upregulated in both circulation and liver [19], and blocking RANKL signaling in liver improves liver insulin resistance in HFD mice, suggesting that RANKL plays an important role in the pathogenesis of NAFLD [20]. In bone, RANKL binds to RANK on the surface of osteoclast precursors to promote osteoclast generation and bone resorption, while OPG, a trick receptor, inhibits the intercellular merger of RANKL and RANK, resulting in reduced activity, proliferation and survival of osteoclasts [21, 22]. We found that the serum levels of TNF-α and IL-6 in NAFLD mice increased significantly at 24 weeks, while the level of OPG mRNA in bone tissue decreased significantly and the level of RANKL mRNA increased significantly. Therefore, it can be seen that TNF-α and IL-6 may affect osteoclast function and lead to osteoporosis through the OPG/RANK/RANKL axis. However, the levels of TNF-α and IL-6 did not increased more at 32 weeks than that at 24 weeks. Differently, the changes in metaphyseal structural parameters and BMD were more evident at 32 weeks. Therefore, we considered that there might be other factors that influence bone structure changes in the progressive stages of NAFLD.

Previous evidence has demonstrated that patients with NAFLD have lower IGF-1 level than healthy controls and show a negative correlation between histological severity of NAFLD and IGF-1 level [23]. In 6- and 19-month-old mice, IGF-1 from liver has been shown to be necessary for maintaining cortical bone mass, and the lack of endocrine IGF-1 leads to elevated cortical porosity [24]. Nevertheless, the main principle of IGF-1 affecting bone structure in NAFLD has not been completely understood. We found that serum IGF-1 levels decreased at 24 weeks and were more pronounced at 32 weeks, along with significant decreases in Runx2 mRNA and OSX mRNA levels, which were consistent with BMD changes.

Runx2 is specifically elevated in hepatic stellate cells (mHSC) of NAFLD mice and accelerates the evolution of NAFLD to NASH by inducing macrophage migration in vitro [19]. Meanwhile, Runx2 plays a decisive role in the osteoblastic differentiation from bone marrow mesenchymal stem cells [25]. IGF-1 can activate the MAPK pathway, up-regulate Runx2 mRNA expression, increase the activity of Runx2 [26], and has the ability to promote osteoblast proliferation, differentiation and coupling matrix mineralization [27]. Osx (Osterix) is considered as a downstream target of Runx2, promoting the differentiation of mesenchymal progenitor cells and initiating osteogenesis during osteogenesis, while Osx promotes the maturation of functional osteoblasts [28]. In addition to up-regulating Runx2, IGF-1 also significantly affects the level of OSX and promotes the expression of osteoblast marker genes [29]. It can be seen that the change of IGF-1 signaling pathway affects the expression of Runx2 and OSX and plays an important role in the liver fibrosis stage of NAFLD. However, IGF-1 secreted from the liver is reported to exert a little influence on the growth of cortical periosteal bone and adult axial skeletal, and it is not needed for maintaining the growth of trabecular bone of adult mice [30].

Interestingly, we found that the IGFBP-1 level was significantly increased at 32 weeks. IGFBP-1 is mainly generated by liver cells and is a soluble binding proteins (6 types in total) that controls the bioavailability of IGF-1 via specifically binding to IGF-1 [31]. A pilot study found that there was a close relationship between serum IGF-1 and IGFBP-1 levels and advancement of liver fibrosis of NAFLD [32]. The blood IGFBP-1 was capable of crossing the capillary barrier to exert direct function from cellular perspective [33]. It means that high IGFBP-1 level in the serum indicates high level of IGFBP-1 in the bone [34]. IGFBP-1 binds to integrin-β on the precursor membrane of osteoclasts and enhances RANKL-mediated osteoclast activation and proliferation, leading to bone loss [35]. Therefore, the bone microstructural and BMD changes in NAFLD during the progressive stage were related to IGF-1 and IGFBP-1 changes.

It was reported that diet supplemented vitamin D could improve its own status and could also alleviate disease parameters such as inflammatory, metabolic, and chemical parameters in NAFLD patients [36]. Although low vitamin D level in serum is related to fibrosis and insulin resistance in hepatocytes, while it is not related to bone health [37]. Therefore, it is not clear whether vitamin D affects bone structure in NAFLD.

Conclusion

To be concluded, this study explored the changes of microstructure of bone over time by micro-CT in a mouse model of NAFLD induced by a high-fat diet. It was found that: (1) Bone loss and the alternations of bone microstructure and BMD occurred in parallel with the progression of NAFLD in HFD-fed mice; (2) Bone structural parameters had no obvious alternations during the 'first hit' stage of NAFLD (at 16 weeks). Changes of the inflammatory cytokines TNF-α and IL-6 can induce enhanced osteoclast function through the OPG/RANK/RANKL signaling pathway and may be critical for changes in bone microstructure and BMD during the "second hit" phase of NAFLD (at 24 weeks). Bone microstructural and BMD changes during the progressive stage in NAFLD were related to IGF-1 and IGFBP-1 levels, which reduces the mRNA expressions of Runx and OSX, resulting in decreased osteoblast function (at 32 weeks). As one of the most common chronic liver disorders, the etiology of NAFLD has been intensively studied in patients with increased bone loss regardless of age or gender. Further studies are needed to investigate how liver diseases influence bone metabolism, and our study may bring a new insight to defeat the two intractable diseases including osteoporosis and NAFLD.

Limitations

This experimental study has only been verified at the animal level, and further exploration at the cellular level will be carried out in the next step.

Abbreviations

NAFLD	Nonalcoholic fatty liver disease
NASH	Nonalcoholic steatohepatitis
HFD	High-fat diet
WT	Wild-type
micro-CT	Micro-computed tomography
TNF-α	Cytokines tumor necrosis factor-α
IL-6	Interleukin-6
IGF-1	Insulin-like growth factor-1
IGFBP-1	Insulin-like growth factor binding protein-1
ALT	Alanine transaminase
GLU	Serum glucose
AST	Aspartate aminotransferase
TC	Total cholesterol
TG	Triglycerides
IR	Insulin resistance
Tb.Sp	Rabecular separation
BV/TV	Bone volume ratio
Tb.Th	Trabecular thickness
Tb.N	Trabecular number
Conn.D	Connectivity density
C.Th	Cortical thickness
BMD	Bone mineral density
tBMD	Tissue BMD
vBMD	Volumetric BMD
ELISA	Enzyme-linked immunosorbent assay
25(OH)D	25-Hydroxyvitamin D

Wang *et al. Journal of Orthopaedic Surgery and Research*   (2023) 18:915

Page 10 of 11

OPG	Osteoprotegerin
RANK	Receptor activator of nuclear factor kappa-B
RANKL	Receptor activator of nuclear factor kappa-bligant
Runx2	Runt-related transcription factor 2
Osx	Osterix
CTX-I	C-terminal crosslinked telopeptides of type I collagen
TRAP	Tartrate resistant acid phosphatase
PINP	N-terminal propeptide of type I procollagen
ALP	Alkaline phosphatase

Author contributions
Designing and performing experiments were contributed by T-HW, J-BL, J-XZ, S-ZG. Analyzing data and writing the paper were contributed by T-HW, Y-GT, X-DL. All authors read and approved the final manuscript.

Declarations

Competing interests
The authors declare no competing interests.

Author details
[1]Department of Orthopedics, The Third Central Hospital of Tianjin; The Third Central Clinical College of Tianjin Medical University; Tianjin Key Laboratory of Extracorporeal Life Support for Critical Diseases; Artificial Cell Engineering Technology Research Center, Tianjin; Tianjin Institute of Hepatobiliary Disease, 83 Jintang Road, Hedong District, Tianjin 300170, China. [2]Department of Hepatobiliary Surgery, The Third Central Hospital of Tianjin; Tianjin Key Laboratory of Extracorporeal Life Support for Critical Diseases; Artificial Cell Engineering Technology Research Center, Tianjin; Tianjin Institute of Hepatobiliary Disease, Tianjin 300170, China.

References
1. Poggiogalle E, Donini LM, Lenzi A, et al. Nonalcoholic fatty liver disease connections with fat-free tissues: a focus on bone and skeletal muscle. World J Gastroenterol. 2017;23:1747–57.
2. Polyzos SA, Anastasilakis AD, Efstathiadou ZA, et al. Postmenopausal osteoporosis coexisting with other metabolic diseases: treatment considerations. Maturitas. 2021;147:19–25.
3. Chen HJ, Yang HY, Hsueh KC, et al. Increased risk of osteoporosis in patients with nonalcoholic fatty liver disease: a population-based retrospective cohort study. Medicine. 2018;97:e12835.
4. Mantovani A, Sani E, Fassio A, et al. Association between non-alcoholic fatty liver disease and bone turnover biomarkers in post-menopausal women with type 2 diabetes. Diabetes Metab. 2019;45:347–55.
5. Shapses SA, Sukumar D. Bone metabolism in obesity and weight loss. Annu Rev Nutr. 2012;32:287–309.
6. López-Peralta S, Romero-Velarde E, Vásquez-Garibay EM, et al. Bone mineral density and body composition in normal weight, overweight and obese children. BMC Pediatr. 2022;22(1):249.
7. Kaya M, Işık D, Beştaş R, Evliyaoğlu O, et al. Increased bone mineral density in patients with nonalcoholic steatohepatitis. Word J Hepatol. 2013;5:627–34.
8. Reid AE. Nonalcoholic steatohepatitis. Gastroenterology. 2001;121:710–23.
9. Carter LE, Kilroy G, Gimble JM, et al. An improved method for isolation of RNA from bone. BMC Biotechnol. 2012;12:5.
10. Upala S, Jaruvongvanich V, Wijarnpreecha K, et al. Nonalcoholic fatty liver disease and osteoporosis: a systematic review and meta-analysis. J Bone Miner Metab. 2017;35:685–93.
11. Gautam J, Choudhary D, Khedgikar V, et al. Micro-architectural changes in cancellous bone differ in female and male C57BL/6 mice with high-fat diet-induced low bone mineral density. Br J Nutr. 2014;111:1811–21.
12. Li X, Wang Z, Klaunig JE. Modulation of xenobiotic nuclear receptors in high-fat diet induced non-alcoholic fatty liver disease. Toxicology. 2018;410:199–213.
13. Chen DZ, Xu QM, Wu XX, et al. The combined effect of nonalcoholic fatty liver disease and metabolic syndrome on osteoporosis in postmenopausal females in Eastern China. Int J Endocrinol. 2018;2018:2314769.
14. Kurt Z, Barrere-Cain R, LaGuardia J, et al. Tissue-specific pathways and networks underlying sexual dimorphism in non-alcoholic fatty liver disease. Biol Sex Differ. 2018;9(1):46.
15. Chen Z, Yu R, Xiong Y, et al. A vicious circle between insulin resistance and inflammation in nonalcoholic fatty liver disease. Lipids Health Dis. 2017;16(1):203.
16. Hadinia A, Doustimotlagh AH, Goodarzi HR, et al. Circulating levels of pro-inflammatory cytokines in patients with nonalcoholic fatty liver disease and non-alcoholic steatohepatitis. Iran J Immunol. 2019;16:327–33.
17. Yan L, Hu R, Tu S, et al. Meta-analysis of association between IL-6 -634C/G polymorphism and osteoporosis. Genet Mol Res. 2015;14(4):19225–32.
18. De Vries TJ, El Bakkali I, Kamradt T, et al. What are the peripheral blood determinants for increased osteoclast formation in the various inflammatory diseases associated with bone loss. Front Immunol. 2019;10:505.
19. Zhong L, Yuan J, Huang L, et al. RANKL is involved in Runx2-triggered hepatic infiltration of macrophages in mice with NAFLD induced by a high-fat diet. Biomed Res Int. 2020;2020:6953421.
20. Nikseresht M, Azarmehr N, Arya A. Circulating mRNA and plasma levels of osteoprotegerin and receptor activator of NF-κB ligand in nonalcoholic fatty liver disease. Biotechnol Appl Biochem. 2021;68(6):1243–9.
21. Lv YJ, Wei QZ, Zhang YC, et al. Low-dose cadmium exposure acts on rat mesenchymal stem cells via RANKL/OPG and downregulate osteogenic differentiation genes. Environ Pollut. 2019;249:620–8.
22. Theoleyre S, Wittrant Y, Tat SK, et al. The molecular triad OPG/RANK/RANKL: involvement in the orchestration of pathophysiological bone remodeling. Cytokine Growth Factor Rev. 2004;15(6):457–75.
23. Sumida Y, Yonei Y, Tanaka S, et al. Lower levels of insulin-like growth factor-1 standard deviation score are associated with histological severity of non-alcoholic fatty liver disease. Hepatol Res. 2015;45:771–81.
24. Svensson J, Windahl SH, Saxon L, et al. Liver-derived IGF-I regulates cortical bone mass but is dispensable for the osteogenic response to mechanical loading in female mice. Am J Physiol Endocrinol Metab. 2016;311:E138–44.
25. Komori T. Runx2, an inducer of osteoblast and chondrocyte differentiation. Histochem Cell Biol. 2018;149:313–23.
26. Yuan Z, Zhang T, Cai J. Research progress on the relationship between gut microbiota, IGF-1 and bone metabolism. Chin J Osteoporos. 2021;27(4):599–604.
27. Yan J, Herzog JW, Tsang K, et al. Gut microbiota induce IGF-1 and promote bone formation and growth. Proc Natl Acad Sci USA. 2016;113(47):E7554–63.
28. Chan WCW, Tan Z, To MKT, et al. Regulation and role of transcription factors in osteogenesis. Int J Mol Sci. 2021;22(11):5445.
29. Zhang W, Wang N, Yang M. Periosteum and development of the tissue-engineered periosteum for guided bone regeneration. J Orthop Translat. 2022;33:41–54.
30. Sjögren K, Sheng M, Movérare S, et al. Effects of liver-derived insulin-like growth factor I on bone metabolism in mice. J Bone Miner Res. 2002;17:1977–87.
31. Binoux M. Insulin-like growth factor binding proteins (IGFBPs): physiological and clinical implications. J Pediatr Endocrinol Metab. 1996;9:285–8.
32. Hagström H, Stål P, Hultcrantz R, et al. IGFBP-1 and IGF-I as markers for advanced fibrosis in NAFLD-a pilot study. Scand J Gastroenterol. 2017;52:1427–34.
33. Kelley KM, Oh Y, Gargosky SE, et al. Insulin-like growth factor-binding proteins (IGFBPs) and their regulatory dynamics. Int J Biochem Cell Biol. 1996;28:619–37.
34. Lundin H, Sääf M, Strender LE, et al. High serum insulin-like growth factor-binding protein 1 (IGFBP-1) is associated with high fracture risk

independent of insulin-like growth factor 1 (IGF-I). Calcif Tissue Int. 2016;99(4):333–9.

35. Lee SY, Fam KD, Chia KL, et al. Age-related bone loss is associated with FGF21 but not IGFBP1 in healthy adults. Exp Physiol. 2020;105(4):622–31.

36. Hussain M, Iqbal J, Malik SA, et al. Effect of vitamin D supplementation on various parameters in non-alcoholic fatty liver disease patients. Pak J Pharm Sci. 2019;32:1343–8.

37. Chang EJ, Yi DY, Yang HR. Vitamin D status and bone mineral density in obese children with nonalcoholic fatty liver disease. J Korean Med Sci. 2015;30:1821–7.

Publisher's Note

Springer Nature remains neutral with regard to jurisdictional claims in published maps and institutional affiliations.